Journal of Visualization, Vol. 11, No. 3 (2008)257-264

Regular Paper

The Flow Induced by a Jellyfish

Ichikawa, S.*[1] and Mochizuki, O.*[2]

*1 Graduate School of Engineering, Toyo University, 2100Kujirai, Kawagoe, Saitama, 350-8585, Japan.
E-mail: dn0700049@toyonet.toyo.ac.jp
*2 Faculty of Engineering, Toyo University, 2100Kujirai, Kawagoe, Saitama, 350-8585, Japan.

Received 30 May 2007
Revised 29 February 2008

Abstract : The purpose of this study is to understand the propulsion mechanism of a jellyfish during its swimming. We observed the motion of a jellyfish (*Aurelia aurita*) by a motion-capture camera, and measured the vector field of flow around a jellyfish by using a PIV (Particle Image Velocimetry) measurement. A jellyfish is considered to be principally propelled by a jet at the contracting phase of its motion. If that is true, it is interesting that a jellyfish never stops traveling even at the expanding phase. We found that a vortex ring with the opposite vorticity to shed vortex ring was inside a jellyfish body in the expanding phase. We discussed a cause of an increase in thrust force and keeping constant speed in the expanding phase.

Keywords : Jellyfish, Motion, Vortex ring, Trust, Particle Image Particle Image Velocimetry Velocimetry (PIV).

1. Nomenclature

Jellyfish	: Aurelia aurita
R	: Maximum diameter of a skirt of a jellyfish
U	: Moving speed at a top position of a jellyfish
f	: Flapping frequency
Re	: Reynolds number based on U, R and ν
ν	: Kinematic viscosity of salt water
A	: Projected area of a jellyfish
R	: Radius of A
M	: Mass and added mass of a jellyfish
ρ	: Density of salt water
D_s	: Shape drag ($=C_D(1/2)\rho U^2 A$)
T	: Thrust
D_f	: Friction drag
C_D	: Shape drag coefficient

2. Introduction

The swimming motion of a jellyfish is elegant and complex in spite of the simple components of its body; it is actually 98 % of its body is water (Azuma, 1980 and 1997). The swimming motion of the jellyfish consists of the expanding motion and contracting motion of the skirt (McHenry and Jed, 2003). The thrust generated by the jet in the contracting motion was predicted to be larger than that

generated by the paddling. The locomotive forces necessary to sustain forward motion were discussed by the momentum theory (Dabiri, 2005) in the wake of a jellyfish and interaction between vortex rings generated by the jet (Dabiri et al., 2005). Their discussion is based on the jet propulsion. However, it is not enough to explain mechanisms of generating thrust in both the expanding and contracting motion.

The swimming motion of a jellyfish is called scissors kick motion. We observed change in speed of the body by using a motion-capture camera. When we compared the change in speed of the body with edge motion, we found that the acceleration occurred in the last stage of the expanding motion. This is not common-sense because it is popular to think that the acceleration occurs in the contracting motion like as the jet propulsion of a squid. Since it is difficult to think the propulsion only from its motion, the flow around a jellyfish during its free swimming was measured by a PIV method. The PIV measurements of free-swimming aquatic animal were for loach and Siddiqui (2007). Released vortices from a caudal fin motion of a free swimming loach were measured by a PIV method by Nagayama et al. (2006). The generated vortices were contributed to propulsion and reduction of flow resistance. Velocity measurements around a freely swimming fish were carried out by Siddiqui (2007). The detection scheme of the fish body was developed by using an image processing and velocity fields were measured by using a PIV method. It is common understanding that propulsion is produced by a jet flow due to alternate vortices released from a two-dimensional motion of a caudal fin for free swimming fish. A vortex ring which is needless to say three-dimensional was found to be released from an edge of a skirt of a jellyfish at the last stage of the expanding motion in our PIV measurements. Since a vortex ring induces a jet type flow by itself, a vortex ring was generated by only one snappy motion of the edge of the skirt. This is different from a fish motion. We present the relation between vortex rings and motions of a jellyfish, and discuss the mechanism of generation of propulsion during the swimming of a jellyfish in this paper.

3. Experimental Setup and Method

In our experiments, a well-known jellyfish is called a moon jellyfish (*Aurelia aurita*) with 46.6 mm in diameter. Since the body is translucent, that type of jellyfish is suitable for flow visualization both around it as well as inside its skirt. Figure 1 shows an experimental setup to visualize a motion and induced flow. We used the water tank with 150 mm in depth, 150 mm in width and 50 mm in length so that the jellyfish swam on a vertical plane. The temperature of salt water was 20 degrees Celsius to keep the experimental conditions as same as the jellyfish's living conditions. We used a high-speed camera "REDLAKEMASD" to observe the motion and flow field around the jellyfish. Since the motion of the jellyfish is slow, we set frame rate of the high-speed camera 60FPS. We used a metal halide lamp as a light source. To see the motion in the center section of the jellyfish, we illuminated the section by a 1.5 mm thick light sheet with.

We used carcasses of animal plankton as tracers for flow visualization around the jellyfish. The plankton is harmless to the jellyfish because it is food. At first, we tried an artificial particle but the jellyfish got weak and did not swim anyway. Thus, we used the plankton to save the jellyfish from the damage and stress caused by the particles. The plankton is called *Artemia Salina*, or "brine shrimp" in common. Its density is almost equal to that of salt water, so that it suspends in salt water and follows the flow well. The average size of the plankton was about 200 μm. When the jellyfish was put in the test water tank including the plankton, it releases slime because it recognizes the plankton as food. Since the slime lumps the plankton together, we need to remove the slime by using a dropping pipette before recording the flow around the jellyfish. We analyzed the motion taken by the high-speed camera by a software "DIPP MOTION 2D" supplied by DITECT Co. Ltd. We traced three representative points at every frame of the movie to obtain the speed of the motion. We used the analysis software "DIPPFLOW" by DITECT Co. Lt for PIV measurements to obtain the flow field around the jellyfish.

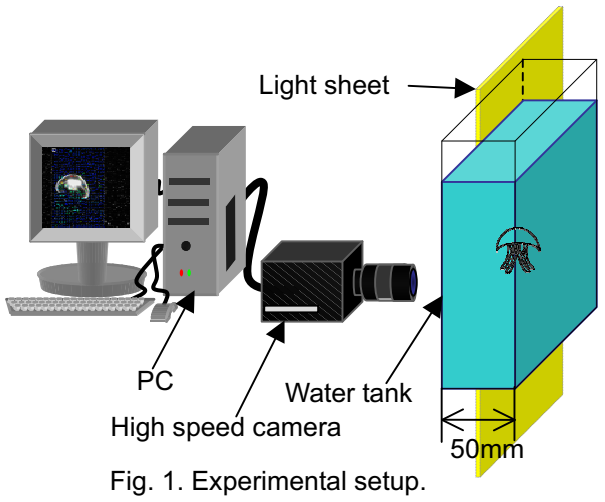

Fig. 1. Experimental setup.

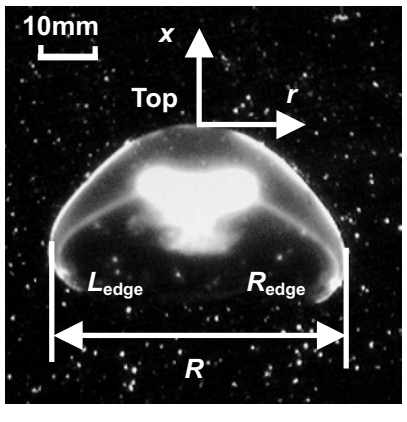

Fig. 2. Definition of symbols and coordinates.

Definition of symbols

Figure 2 shows the longitudinal section of the jellyfish illuminated by the light sheet. A characteristic length was defined by the maximum diameter of the body, R, in the expanding phase during swimming. In this experiment, R was 46.6 mm. The origin of the coordinates was located on the top. The left edge of the skirt was denoted by L_{edge}, and the right edge of the skirt R_{edge}. The speed at the three points was calculated from the distance when they moved between consecutive frames. The traveling direction of the jellyfish was defined by the x-direction. The radial direction, perpendicular to x, was denoted by r.

4. Results

Figure 3 shows loci of the reference points on the jellyfish during 4 cycles of the flapping motion. The contracting and expanding motion of the skirt propels the jellyfish forward. The skirt-motion is periodic, and is called "flapping". This motion took 1.1 sec for contracting, and 0.42 sec for expanding. Therefore, one flapping period was 1.52 sec. The flapping frequency, f, is 0.66 Hz so that the reduced frequency, as defined by $2\pi fR/U$ is 14. This shows that the unsteadiness governs the flow induced by the jellyfish. The jellyfish was traveling for 18 mm in distance during one flapping period. This distance is equivalent to $0.4R$.

The change in distance measured from the starting point for three reference points is shown in Fig. 4. This shows the result of 4 cycles flapping. The solid line represents the locus distance of the "Top" which represent the body and the broken lines represent the locus distance of the edges denoted by L_{edge} and R_{edge}. The increasing ratio of the moving distance of the "Top", that is the body, point to time is the representative speed, U, of the body, which is 13.6 mm/s. An increase in distance of the edges of the skirt is almost twice as large as that of the body.

The change in speed is estimated by differentiating the data given in Fig. 4. The result is shown in Fig. 5. A solid line represents the speed at the body and broken lines the speed of the edges. The speed of the top varies periodically. The maximum speed is about 20 mm/s and the minimum speed is about 10 mm/s. The minimum speed is almost kept constant during a half period of the swimming. In contrast to this, the speed of the edge observed from a fixed coordinates is almost twice of the body speed. Taking into account the speed of the body, the relative speed at the edges is almost the same as the moving speed of the body. The Reynolds number, $R_e=RU/\nu$ is 511. Here, ν is the kinematics viscosity of salt water. This value is relatively small, but the friction force can not be ignored. The maximum cross correlation coefficient between the changes in speed of the top and R_{edge} was 0.92 at -0.05 sec. This means that the speed of the edge attained the maximum before the speed

of the top attained maximum. The period, T, of the change in speed of the top and R_{edge} is about 1.4 sec, that is the same value as the observation by the movie.

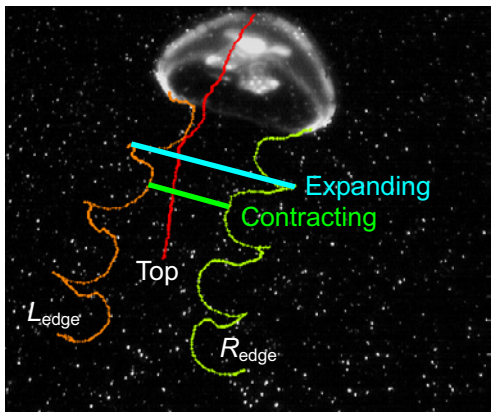

Fig. 3. Loci of points Top, R_{edge} and L_{edge}.

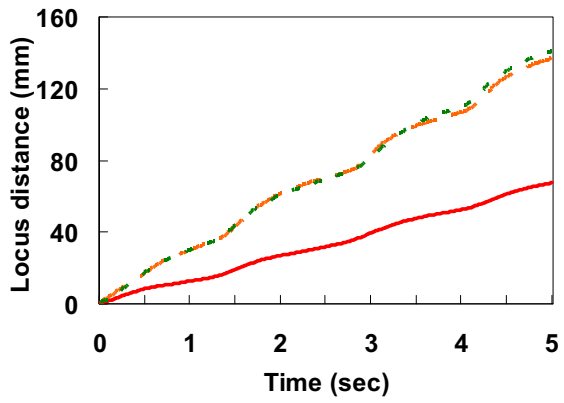

Fig. 4. Locus distance of points Top, L_{edge} and R_{edge} from each starting point, Solid line:Top, Broken line:edges.

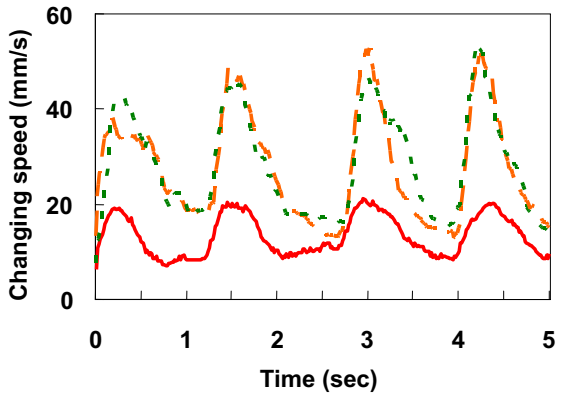

Fig. 5. Change in speed at Top, L_{edge} and R_{edge}, Solid line:Top, Broken line:edges.

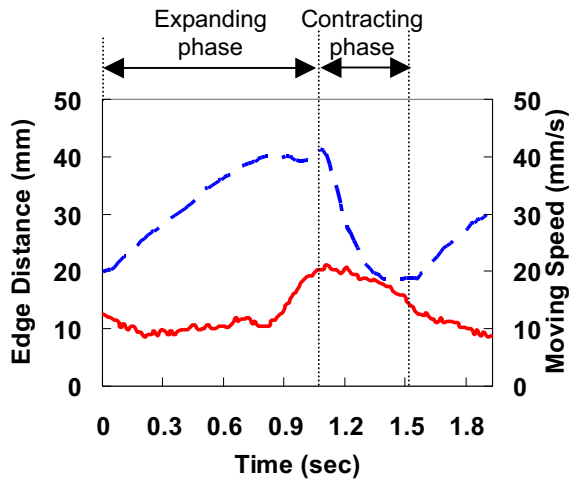

Fig. 6. Change in distance between L_{edge} and R_{edge}, Solid line:Moving velocity of Top, Broken line:Edge distance.

The changes in the speed of the body and the interval of the edges are plotted by solid line and broken lines respectively against time in Fig. 6. The time interval related to the contracting phase is 0.38 seconds, whereas the time interval related to the expanding phase is 0.94 seconds. Thus, the contracting phase is about 30 % of one swimming period and the expanding phase about 70 %. This means that the jellyfish contracts the skirt quickly, and expands the skirt slowly. It is interesting that the speed of the body accelerates at the last stage of the expanding phase and the speed of the body decelerates at the contracting phase. The drag should increase when the skirt is expanded, because of the projective area increases. However, the speed of the body stays constant after the minimum velocity and a steep rise at the end of the expanding phase. This fact is unexpected. If a generation mechanism of thrust of the jellyfish is analogous to that of a squid, acceleration must occur at the contracting phase. The result presented in Fig. 6 shows that the thrust is generated all time. This will be discussed later by considering the change in volume inside of the skirt. The cross correlation coefficient calculated between the changes shown in Fig. 6 attains a positive maximum value, 0.83, at -0.3 sec, and the negative maximum value, -0.90, at 0.3 sec. This means that the distance between the edges of the skirt becomes the maximum before the speed of the body attains

the maximum, and it becomes the minimum after the speed of the body attains the maximum.

Figure 7 shows the change in the inside volume of the skirt to speed of the body. The solid line represents the change in speed at the body and the broken line represents the change in volume of the inside skirt. The volume was obtained as the inside area of the skirt of the 1 mm thickness. The inside area was measured by the image processing of the picture. We used the software "Scion Image" supplied by Scion Co. Ltd. for image processing to calculate changing in volume inside the skirt obtained from the movie. The data show that the volume increases in the expanding phase and attains the maximum volume at the beginning of the increase of the speed of the body. The speed of the body starts to increase as the volume decreases; a jet is ejected at this time, and the jellyfish thus obtains thrust power as the reaction of ejection. The speed of the body attains the maximum during the ejection. If we define the contracting and expanding phase according to the change in volume, the time interval of each phase is almost the same. In this case, the time when the speed of the body shows constant is coincident with the time interval of the suction. The cross correlation between the speed of the body and change in volume attains the positive maximum value, 0.76, at -0.33 sec. The cross correlation coefficient attains the negative maximum value, -0.88, at 0.35 sec. This means that the volume of the inside skirt becomes the maximum before the speed of the body attains the maximum and it becomes the minimum after the speed of the body attains the maximum.

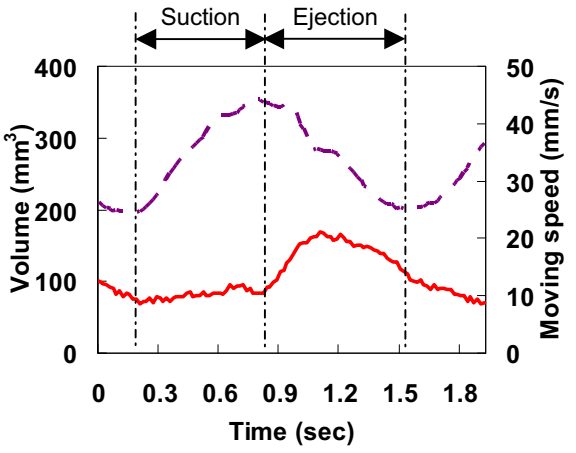

Fig. 7. Change in volume inside of the skirt, Solid line:Moving velocity of Top, Broken line:Changing volume.

There are two questions about the change in the speed of the body. One is why the speed is kept constant during the expanding phase, and the other is why the speed decreases even if the jet ejects. To understand these phenomena, we estimated the balance between the shape drag and inertial force. Forces acting on the bell-shape body that is a model of the jellyfish are shown in Fig. 8. The equation of motion is given by Eq. (1). The shape drag, D_s , is given by Eq. (2).

$$F = m\frac{\partial U}{\partial t} = T - D_s - D_f \tag{1}$$

$$D_s = C_D A\frac{\rho U^2}{2} \tag{2}$$

Here, F is the resultant force estimated by the mass of the jellyfish including the added mass and acceleration obtained by the derivative of U presented in Fig. 6. If C_D is assumed constant, unknown terms are T and D_f, because F and D_s are obtained from the values A, U, m and ρ given by the experimental data. To estimate the shape drag, the area A ($=\pi r^2$) and U are used the experimental data as a function of time. The drag coefficient, C_D, of a bell-shape is adopted a constant value of 0.38 (JSME, 2006). Because of there is no data concerning about the drag coefficient of a bell-shape at Re = 500, we used the value at $Re = 4 \times 10^5$. However, the value of C_D is considered not to be different in this range of Reynolds number according to that of a sphere. The shape drag estimated as the above consideration is smaller than the inertial force by two orders of magnitude. Thus, the change in D_s is negligible in this case. The change in force $F+D_s$. is shown in Fig. 9. Since $F+D_s$ is equivalent to $T-D_f$ from Eq. (1), the graph shows a balance of the thrust and friction force acting on the jellyfish. The force acting on the jellyfish is almost zero during the expanding phase as seen in Fig. 9. This is the result of the constant speed during the expanding phase. Thus, the thrust and friction force are

balanced in this phase. Whereas the thrust exceeds friction force during the first half of the contracting phase, the friction force prevails against the thrust during the latter half of the contracting phase. The flow along the outer wall was accelerated at the latter half of the contracting phase. Since the friction force is proportional to the square of the speed near the wall, the friction force overcomes the trust at this time as shown in Fig. 9.

The flow around the jellyfish during one period of swimming was obtained by a PIV method. The successive frames taken at every 0.30 sec are shown in Fig. 10. Figures 10(1), (2) and (3) are corresponding to the expanding phase and Figs. 10(4), (5) and (6) the contracting phase. The flow along a outer surface turned the round edge and the inside vortex ring started to grow as shown in Fig. 10(6) which is in the last stage of the contracting phase. The influx into the skirt along the center line was observed in the expanding phase as seen in Figs. 10(2) and (3). The velocity of the influx increased because of the growth of the inside vortex ring. The boundary layer flow along the outer wall came into the skirt as to supply the vorticity as shown in Fig. 10(2). The diameter of the inside vortex ring expanded due to the increase width of the skirt. The circulation of the inside

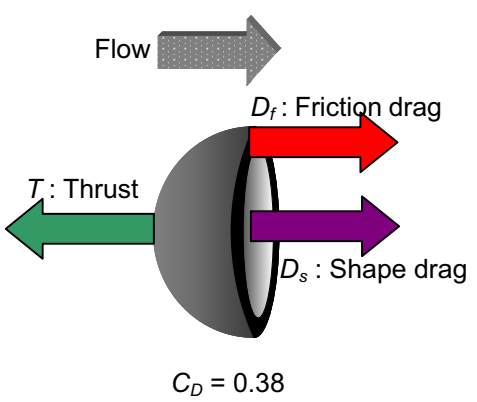

Fig. 8. The model of the drag coefficient and operation force.

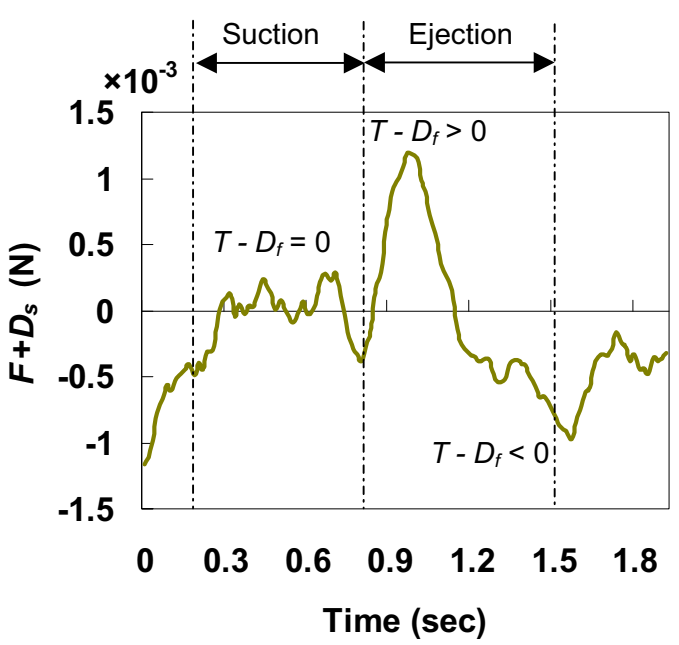

Fig. 9. Change in resultant force during pitching motion.

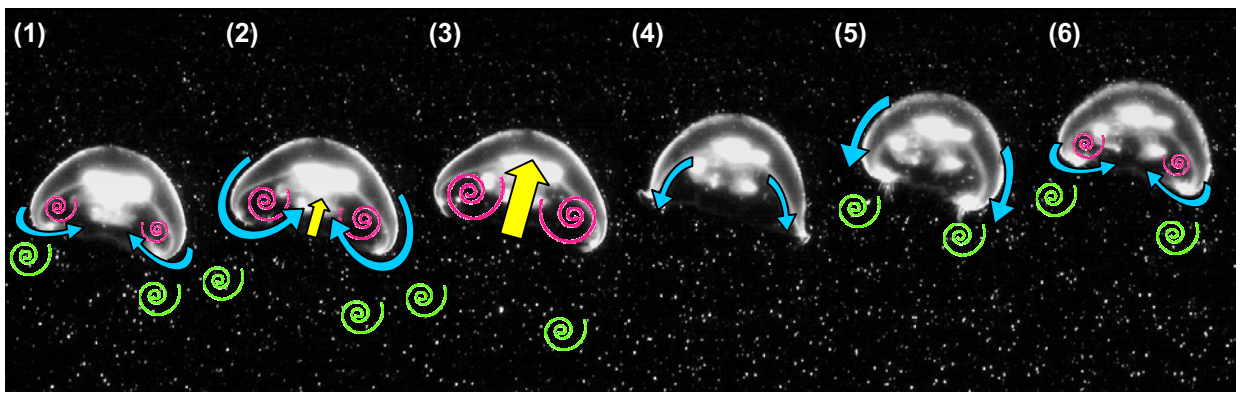

Fig. 10. Swimming and vortices. Time interval is 0.30 sec. Figures (1), (2) and (3) are patterns in expanding phase and Figs. (4), (5) and (6) in contracting phase.

vortex ring increases with increasing the diameter, according to the potential theory of three dimensions. The ratio of increment of the circulation to that of the initial one is 1.06 by using the values of 4.9 mm (0.11*R*), the diameter of the vortex core, and 12.3 mm (0.27*R*), the diameter of the vortex ring, in this experiment. The vortex ring generated inside the skirt is similar to a vortex ring behind a rising vapour bubble observed by Cieslinski et al. (2005). Whereas, a vortex ring with opposite rotation to that of the inside one was released at the timing of Fig. 10(5). This vortex ring is generated at the edge of the skirt by a snappy motion. The flow was induced by the vortex ring and is similar to a jet and a flame vortex observed by Hargrave (2006).

The flow field depicted by path lines is shown in Fig. 11. The inside vortex ring and vortex ring located behind the jellyfish are seen in Fig. 11. The latest one is originated from the tip of the skirt in the contracting phase. These vortex rings show foci and the flow between them shows one at a saddle point. These patterns show that the flow field is a three-dimensional.

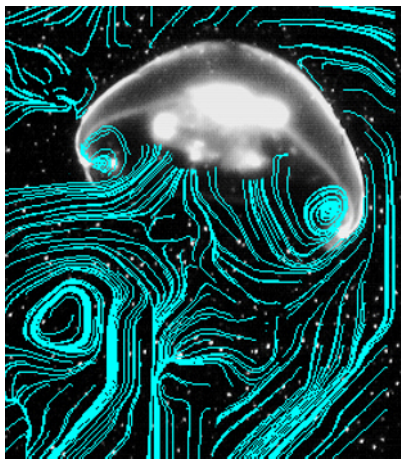

Fig. 11. The path line just before the end of the expanding phase.

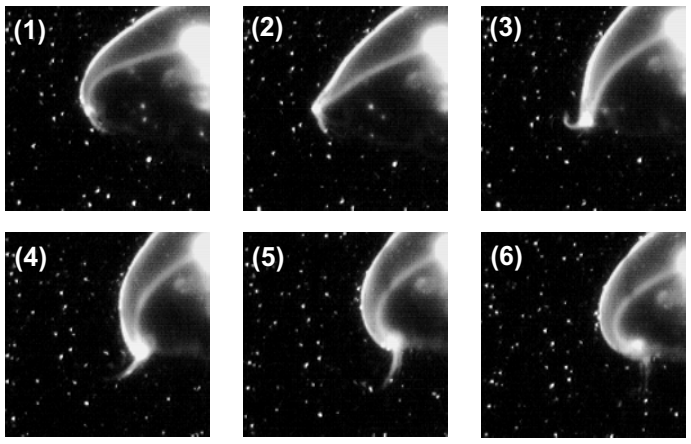

Fig. 12. Snappy swing motion of the skirt, time interval is 0.13 sec.

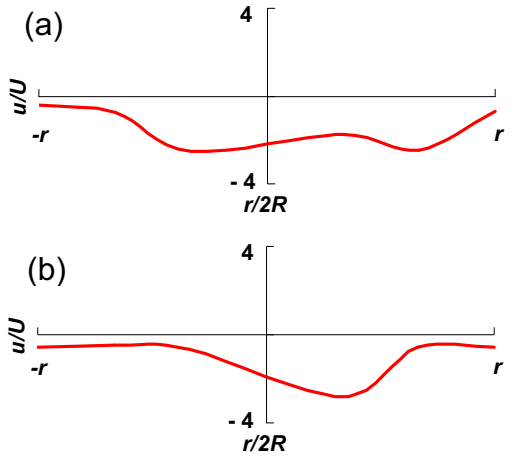

Fig. 13. Velocity distribution measured at (a) the opening located at *x/R* = 0 and (b) the shed vortex ring located at *x/R* = 0.39.

The generation of the vortex ring released from the edge is shown in Fig. 12. This vortex ring looks like a starting vortex at the trailing edge of an impulsive starting wing. Namely, it is supposed to be yielded by a snappy motion to satisfy the Kutta condition at the edge. The snappy motion that is called the paddling motion is shown in Fig. 12 as successive frames taken at every 0.13 sec. The first motion of the snappy swing as seen in Fig. 12(1) started at the beginning of the ejecting phase as shown in Fig. 7. Thus, this timing is still in the expanding phase as compared with the result shown in Fig. 6. The moving velocity attends the maximum at this timing. Figure 12(2) shows at the start of contracting phase, and the distance between edges becomes the maximum. The flow along the outside surface of the skirt toward inside was observed when the tip started to move as shown in Fig. 12(3). The vortex rings started to grow at this timing and was released at the end of ejection phase as shown in Fig. 12(6). From this result, the thrust is concluded to be related to the generation of this vortex ring.

The velocity distribution between L_{edge} and R_{edge} at the contracting phase is shown in Fig. 13(a). The outflow is observed near the edges, and its magnitude is three times larger than the average speed. This out flow is induced by the vortex ring generated at the edge mentioned before. Whereas, the jet-type velocity distribution is observed at the position of the released vortex ring behind the

skirt which is located at x/R = 0.39 (18 mm) as shown in Fig. 13(b). The peak value of the velocity is approximately $3U$. This flow looks like a jet comes from the jellyfish, but this is the induced flow by the released vortex ring. We conclude that the thrust to accelerate is due to the generation of the released vortex ring and thrust to maintain the constant speed of the body is due to the inside vortex ring.

5. Conclusions

We observed the free swimming of a jellyfish by using a motion capture system and measured flow fields around the jellyfish by a PIV measurement with a high-speed CCD camera. The speed of swimming showed almost constant during the expanding phase of the skirt, whereas it increased in the first half period of the contracting phase and decreased in the latter half period of the contracting phase. We estimated the balance of the thrust force and friction force from the measurement of inertia force and estimation of shape drag. It was found that the thrust became the maximum in the ejection phase at which a vortex ring was generated and released from the edge of the skirt. An vortex ring generated inside the skirt contributed to maintain the body speed so as to overcome the drag increment in the expanding phase.

Acknowledgements

We express our gratitude for a support of Special Study Foundation from Toyo University and for a supply of jellyfish from KAMO AQUARIUM to carry on this study.

References

Azuma, A., Storok of organism, Swimming of bacteria to person, (1980), 67-68, Blue Backs (in Japanese).
Azuma, A., Encyclopedia of Organism of Movement, (1997), 146-148, Asakura shoten (in Japanese).
Cieslinski, J. T., Polewski, J. and Szymczyk, J. A., Flow Field around Growing and Rising Vapour Bubble by PIV Measurement. Journal of Visualization, 8-3 (2005), 209-216.
Dabiri J. O., Colin, S.P., Costello, J.H. and Gharib, M., Flow patterns generated by oblate medusan jellyfish: field measurements and laboratory analyses**,** J Exp Biol, 208-7 (2005), 1257-1265.
Dabiri, J. O., On the estimation of swimming and flying forces from wake measurements, J Exp Biol, 208 (2005), 3519-3532.
Hargrave, G. K. and Jarvis, S., A study of Premixed Propagating Flame Vortex Interaction, Journal of Visualization, 9-2 (2006), 179-187.
JSME, Mechanical Engineering Hand book, α4: Fluids Engineering, (2006), 85 (in Japanese).
Matthew, J. McHenry and Jason, Jed, The ontogenetic scaling of hydrodynamics and swimming performance in jellyfish (Aurelia aurita), J Exp Biol, 206 (2003), 4125-4137.
M. H. Kamran Siddiqui, Velocity measurements around a freely swimming fish using PIV ,Meas. Sci. Technol., 18 (2007), 96-105.
Nagayama, K. and Tanaka, K., 2D-PIV Analysis of Loach Motion and Flow Field, Journal of Visualization, 9-4 (2006), 393-401.

Author Profile

Seiji Ichikawa: He received his B.Eng. in Department of Mechanical Engineering in 2005 from Toyo University. He received his M.Eng. in Department of Intelligent Material and Mechatronics System in 2007 from Toyo University Graduate School. He joins in Biomechanical Engineering Laboratory, Toyo University Graduate School since 2004. His research interests are Flow Visualization, PIV and Flow Induced by Aquatic Animal. He is a member of the Japan Society of Fluid Mechanics and American Physical Society.

Osamu Mochizuki: He received his Master of Eng. in Mechanical Engineering in 1984 from Hokkaido University. He also received his Doctor of Engineering in 1987 from Hokkaido University. He worked in Department of Mechanical Engineering, Hokkaido University as an associate professor from 1990 to 2002. He works in Mechanical Engineering and System Robotics, Toyo University as a professor since 2003. His research interests are flow induced by small life, micro air vehicles, bio mimetics, PIV.